Surface & Coatings Technology 372 (2019) 422–426

Contents lists available at ScienceDirect

Surface & Coatings Technology

journal homepage: www.elsevier.com/locate/surfcoat

Corrosion resistance of tartaric-sulfuric acid anodized AA2024-T3 sealed with Ce and protected with hybrid sol–gel coating

M. Terada[a,*], F.M. Queiroz[b,e], D.B.S. Aguiar[c], V.H. Ayusso[a], H. Costenaro[b], M.-G. Olivier[d], H.G. de Melo[b], I. Costa[a]

[a] Nuclear and Energy Research Institute, Av. Lineu Prestes, 2242 São Paulo, SP, Brazil
[b] Polytechnic School of the University of São Paulo, Rua Prof Mello de Moraes, 2463 São Paulo, SP, Brazil
[c] Universidade Estadual de Ponta Grossa, Ponta Grossa, PR, Brazil
[d] University of Mons, Place du Parc, 20 Mons, Belgium
[e] Escola e Faculdade de Tecnologia SENAI, Rua Bento Branco de Andrade Filho, 379, São Paulo, SP, Brazil

ARTICLE INFO

Keywords:
TSA anodizing
AA2024
Ce
Sol-gel coating

ABSTRACT

2024 aluminum alloys are widely used in the aerospace industry due to properties as lightweight, high specific strength and durability. However, they are prone to localized corrosion due to its high amount of intermetallics. A promising method to protect the exposed metal surface is to use eco-friendly alternative corrosion inhibitors in combination with a barrier coating system. In this study, a treatment in an aqueous solution with the addition of cerium ions has been proposed and its effects on the corrosion resistance of the AA2024-T3 alloy were investigated. Samples were anodized, hydrothermally treated in aqueous solutions, containing or not cerium ions at the boiling temperature and then coated with sol-gel. The effect of Ce ions in the characteristics of the surface film formed, such as morphology and corrosion resistance, was investigated by scanning electron microscopy and electrochemical impedance spectroscopy (EIS). The EIS results showed that the addition of Ce(III) ions improved the corrosion resistance of the AA 2024-T3 TSA anodized and hydrothermally treated.

1. Introduction

AA2024-T3 is the most used AA2XXX in the aerospace industry due to its properties as lightweight, high specific strength and durability [1]. Besides, its passive oxide layer provides corrosion resistance as it is formed by a porous and a barrier layer [2–4]. However, its high amount intermetallics diminish its corrosion resistance as they form galvanic couples with the matrix.

Chromic acid anodizing was used in aerospace industry to improve not only the corrosion resistance but also the paint adhesion [5]. However, this process generates hexavalent chromium ions, considered toxic for health [6–7]. In a few years, this process will be prohibited all over the world and must be substituted for new anodizing and sealing processes. Recent studies are pointing towards tartaric-sulfuric acid anodizing (TSA) as an alternative for the corrosion protection of aluminum alloys, including treatments in cerium containing solution [8–11]. This hydrothermal sealing process provides the required corrosion resistance but diminishes the paint adhesion [12]. Another promising method is to seal the porous anodized layer using a sol–gel coating, trying to maintain the adhesion properties.

In this study, hydrothermal treatments in a solution containing cerium ions and a sol-gel coating have been proposed and their effects on the corrosion resistance of the AA2024-T3 alloy were investigated. Samples were anodized, hydrothermally treated in a cerium containing solution and then coated with sol-gel. The effect of Ce(III) ions in the morphology and corrosion resistance of the surface film was investigated by scanning electron microscopy (SEM) and electrochemical impedance spectroscopy (EIS). The EIS results showed that the addition of Ce(III) ions improved the corrosion resistance of the AA 2024-T3 TSA anodized and hydrothermally treated.

2. Materials and methods

The AA2024-T3 was kindly supplied by EMBRAER S.A. Prior to anodizing, samples of the AA2524 with dimensions of 4.5 cm × 5.0 cm × 0.105 cm were degreased by sonication in acetone for 10 min. Surface preparation was carried out by dipping the samples in an alkaline etching solution: NaOH (40 $g{\cdot}L^{-1}$) at 40 °C for 30 s and in

* Corresponding author.
E-mail addresses: maysaterada@uol.com.br (M. Terada), marjorie.olivier@umons.ac.be (M.-G. Olivier), hgdemelo@usp.br (H.G. de Melo), icosta@ipen.br (I. Costa).

https://doi.org/10.1016/j.surfcoat.2019.05.028
Received 14 November 2018; Received in revised form 18 April 2019; Accepted 10 May 2019
Available online 11 May 2019

a chromate-free commercial acid dismutting bath (Turco® Smuttgo-Henkel) at room temperature for 15 s. Between each step of surface preparation, all specimens were thoroughly washed with distilled water.

Samples were then anodized in a tartaric-sulfuric acid bath (TSA) (40 g·L^{-1} H_2SO_4 and 80 g·L^{-1} $C_4H_6O_6$) at 10 V, for 20 min, at 37 °C. After anodizing, some samples were immediately rinsed with distilled water and partially hydrothermally treated for 5 or 10 min in boiling deionized water with the addition of 50 mM of Ce (III) ions. After that, these specimens were coated once with a hybrid organic–inorganic sol–gel layer using a dip-coater, with immersion time of 2 min and withdrawal rate fixed at 100 mm·min^{-1}. The sol–gel solution was prepared by the addition of tetraethoxysilane (TEOS) (20% v/v) and 3-glycidyloxypropyl-trimethoxysilane (GPTMS) (10% v/v) in a mixture of ethanol (10% v/v) and distilled water (58% v/v). The pH was adjusted to 2.3–2.5 by adding acetic acid to the continuously stirred sol-gel solution. Curing was carried out at 150 °C, for 1 h, in a furnace.

A Gamry PCI4/300 potentiostat-frequency response analyzer system was used to evaluate the corrosion resistance of the samples. EIS was carried out in a classical three electrodes arrangement using 3.80 cm^2 area of the specimen as working electrode, Ag/AgCl (+0.197 V vs. SHE) as reference electrode and a platinum plate as counter electrode. EIS measurements were taken at different immersion times at room temperature, in a naturally aerated 0.1 mol·L^{-1} NaCl solution, over a frequency range from 10^5 to 10^{-2} Hz with 10 points per decade using AC signal amplitude of 20 mV (rms). The monitoring of the electrochemical behavior during immersion test was carried out up to 1008 h, corresponding to 6 weeks.

Scanning electron microscopy (SEM) characterization was performed in a Field Emission Gun Microscope FEI Quanta 650.

3. Results

The microstructure of the AA 2024-T3 is presented in Fig. 1. A great amount of precipitates can be noticed, being Al-Cu-Fe-Mg and Al-Cu-Mn [13]. Most of these precipitates are removed before the anodizing process, during pre-treatment. Fig. 2 shows the pores on the surface of the TSA anodized and unsealed sample. Their distribution is irregular despite they can be noticed even at the bottom of the defective areas.

The corrosion resistance of the anodized, hydrothermally treated in a Ce (III) containing solution and coated samples was evaluated by electrochemical impedance spectroscopy. Anodized and unsealed samples were also evaluated for comparison. The results are presented in Figs. 3 to 5. The Bode phase angle diagrams of the anodized and unsealed samples presented two time constants up to 672 h (4 weeks) of immersion in the test solution. The diagrams are very similar up to 168 h (1 week) of immersion in the test solution. However, after 336 h (2 weeks), both peaks were displaced to lower frequencies. The Nyquist

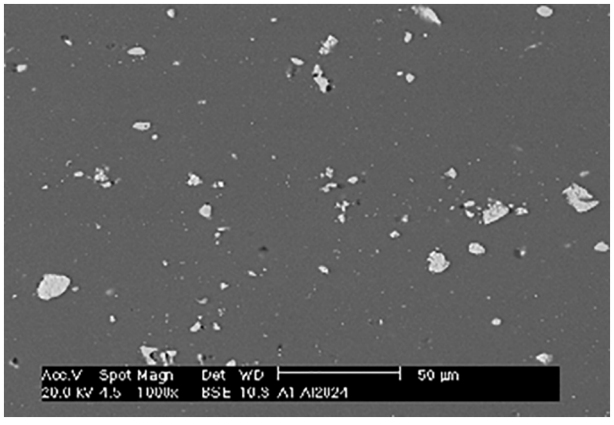

Fig. 1. Micrograph of the AA2024 - T3 surface, as-received sample.

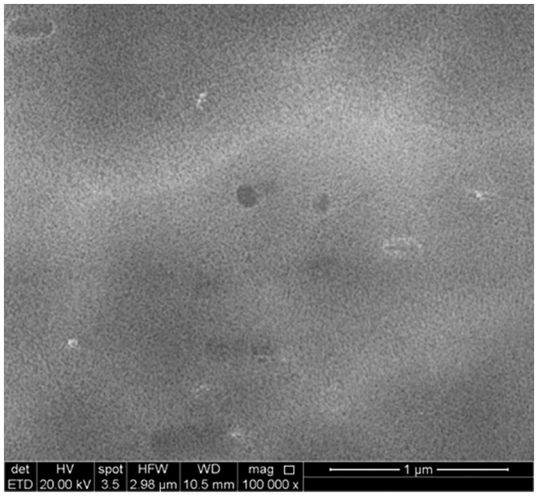

Fig. 2. AA2024 – T3 TSA anodized at 10 V, 37 °C, 20 min. The irregular pores can be seen even inside the defective areas.

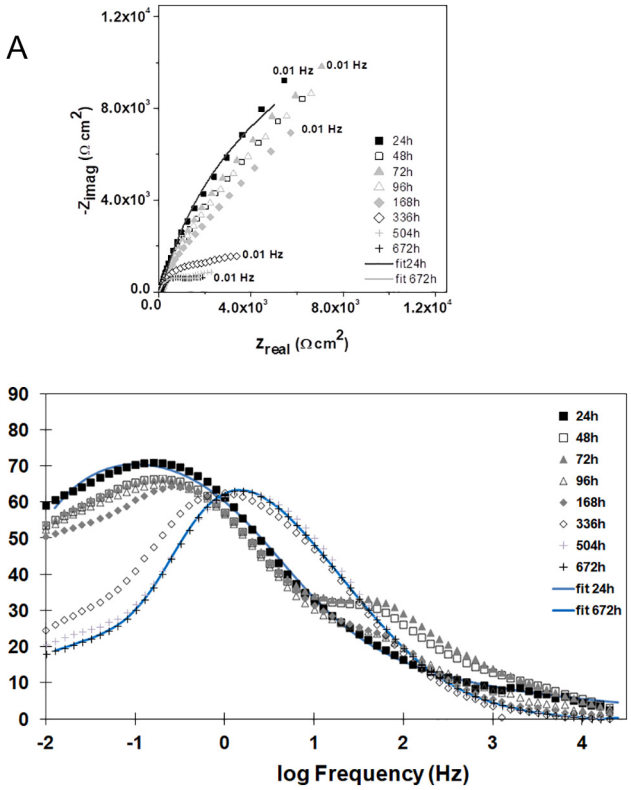

Fig. 3. (a) Nyquist and (b) Bode Phase Angle diagrams of the AA2024 – T3 TSA anodized at 10 V, 37 °C, 20 min. Tests performed in a naturally aerated 0.1 mol·L^{-1} NaCl solution, up to 672 h.

diagrams show that the impedance values decreased after 48 h of immersion and increased after 72 h. After that, the impedance decreases up to 672 h (4 weeks), when these samples were visible corroded.

Samples anodized, hydrothermally treated and coated with sol-gel presented three peaks in the Bode phase diagrams, at higher, medium and lower frequencies. The impedance values are at least two orders of magnitude higher than the ones obtained for the anodized and unsealed samples. Besides, Nyquist diagrams of the anodized, hydrothermally treated and sol-gel coated samples show that the impedance values increased after 336 h (2 weeks) of immersion in the test solution and then decreased gradually up to 1008 h (6 weeks). The EIS results were

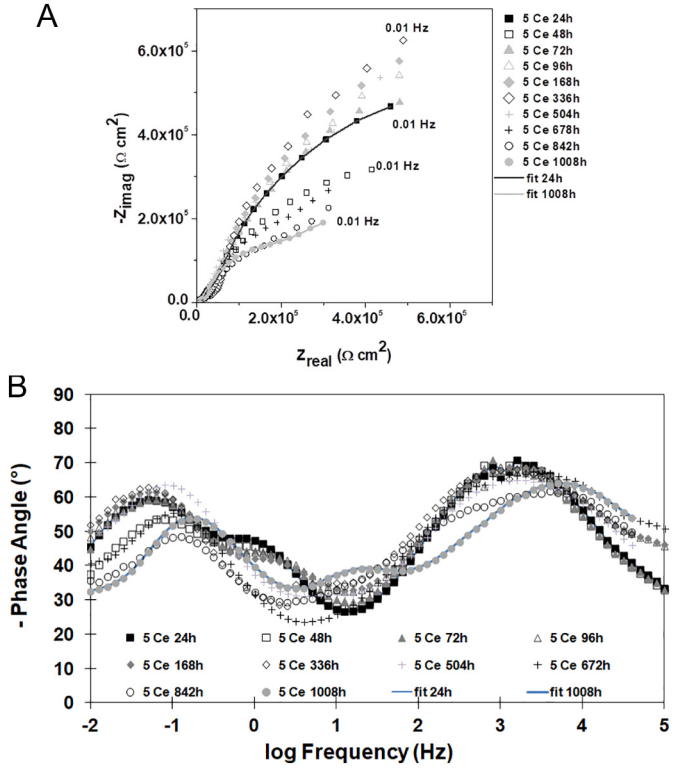

Fig. 4. (a) Nyquist and (b) Bode Phase Angle diagrams of the AA2024 – T3 TSA anodized, hydrothermally treated for 5 min in boiling deionized water with the addition of 50 mM of Ce (III) ions and then sol-gel coated. Tests performed in a naturally aerated 0.1 mol·L^{-1} NaCl solution, up to 1008 h.

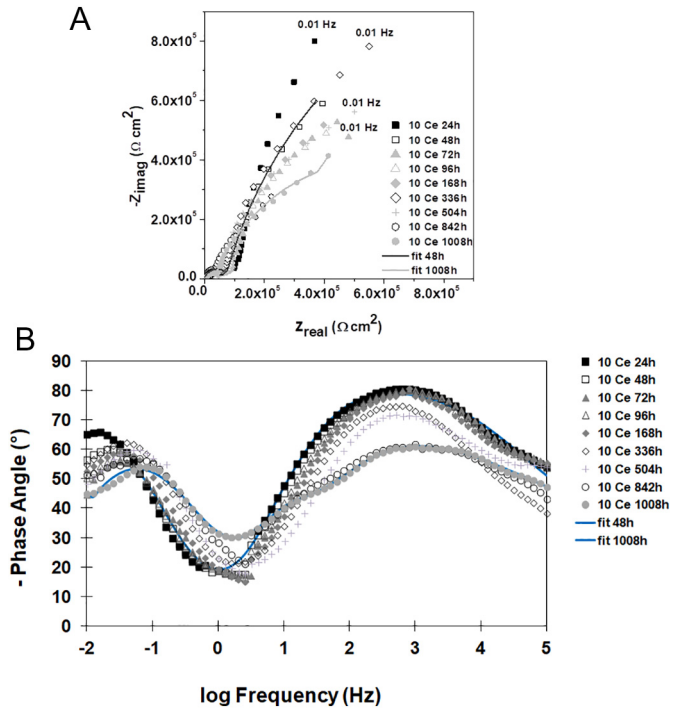

Fig. 5. (a) Nyquist and (b) Bode Phase Angle diagrams of the AA2024 – T3 TSA anodized, hydrothermally treated for 10 min in boiling deionized water with the addition of 50 mM of Ce (III) ions and then sol-gel coated. Tests performed in a naturally aerated 0.1 mol·L^{-1} NaCl solution, up to 1008 h.

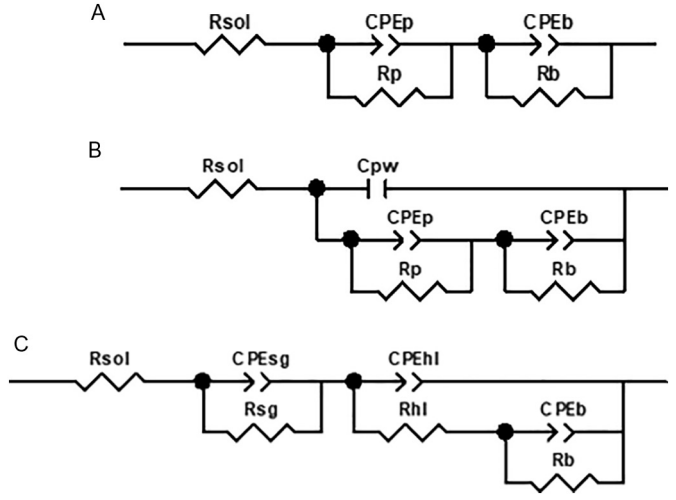

Fig. 6. Electric equivalent circuit fitted to the EIS results of the AA2024-T3 TSA anodized and (a) unsealed, up to 168 h, (b) unsealed, after 168 h of immersion and (c) hydrothermally treated in Ce solution and sol-gel coated.

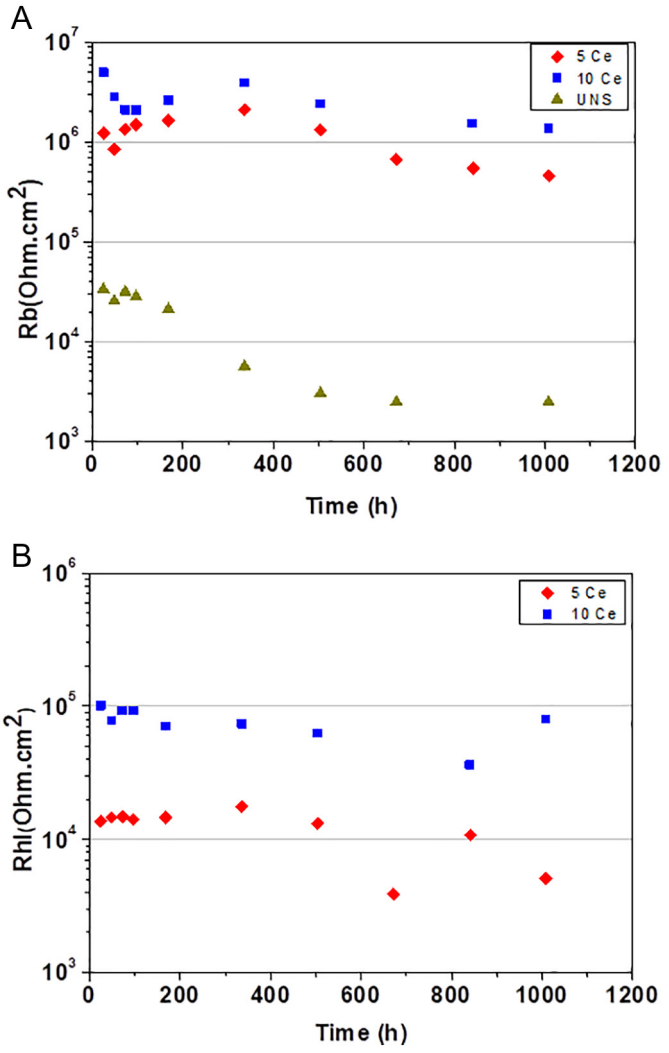

Fig. 7. (a) Rb and (b) Rhl versus immersion time in a naturally aerated 0.1 mol·L^{-1} NaCl solution, up to 1008 h.

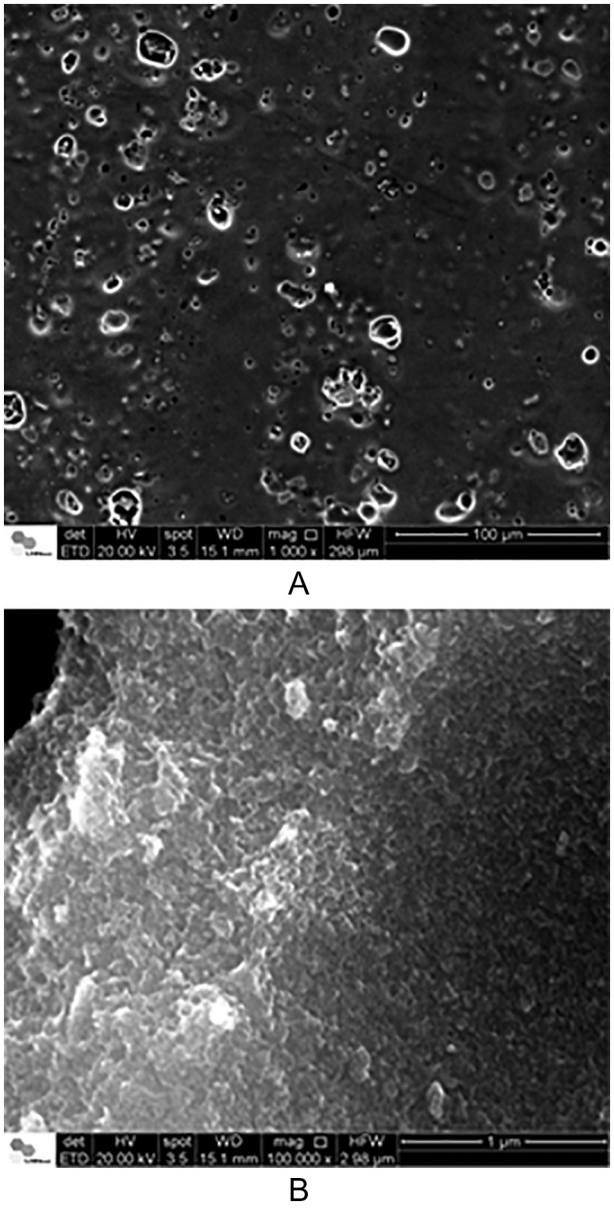

Fig. 8. FESEM images of AA2023-T3 TSA anodized after EIS tests (a) 672 h of immersion in a naturally aerated 0.1 mol·L^{-1} NaCl solution and (b) same at higher magnification.

fitted using electric equivalent circuits – Fig. 6 and the comparative results are shown in Fig. 7. The anodized and unsealed samples were fitted using two R//CPE pairs and the anodized, hydrothermally treated and sol-gel coated samples, using three R//CPE pairs.

After EIS tests, all samples were observed using a scanning electron microscope, and the micrographs are shown in Figs. 8 and 9. The unsealed samples presented a great amount of localized corrosion areas – Fig. 8a and corrosion products can be noticed on their surfaces – Fig. 8b. Some precipitates can be distinguished on the surface of the sol-gel coated samples, below the sol-gel coating, despite the pre-anodizing treatment – Fig. 9. On the other hand, the sol-gel layer can be detected on the surface but micrometric pores can be seen near the intermetallics.

4. Discussion

Figs. 1 and 2 show the surface of the AA2024-T3, respectively in as-received condition and after TSA anodizing. The precipitates must be removed before the anodizing process as they not only affect the morphology of the anodic layer, forming defective porous [14] but also decreases the corrosion resistance.

The electrochemical tests performed to evaluate the corrosion resistance of the anodized and unsealed samples showed the presence of two time constants in the Bode phase angle diagrams. The differences between the Nyquist and Bode phase angle diagrams obtained before and after 336 h (2 weeks) of immersion suggest the presence of corrosion products on the surface of the samples - Fig. 3b. The EIS results were fitted to electric equivalent circuits, presented in Fig. 6. Representative plots are shown in Figs. 3, confirming the accuracy of the fittings. The equivalent circuits fitted to the anodized and unsealed samples are the same proposed by Capelossi et al. [15] – Fig. 6a and b. The porous layer, detected at medium frequencies, is represented by Rp//CPEp and the barrier layer, detected at lower frequencies, by Rb//CPEb. For longer exposure times (superior to 168 h), another element (Cpw) was added to the EIS, related to the pore walls. However, the resistance associated with the pore walls is still very high and do not appear in the equivalent circuit. This component cannot be noticed before 168 h of immersion in the test solution because the impedance associated to the pore walls is extremely high and the impedance of the pores filled with precipitated hydrated alumina is low. The decrease of the barrier layer resistance (Rb), up to one order of magnitude with time of immersion, confirms the loss of surface protection - Fig. 7a. Besides, the micrographic analysis after the EIS tests - Fig. 8 - confirmed that the surface of the samples was corroded.

The presence of three peaks in the Bode phase diagrams of the samples anodized, hydrothermally treated and coated with sol-gel suggests that the high, medium and low frequency time constants can be attributed to the phenomena occurring within the sol-gel coating, the porous layer filled with the sol-gel coating and to the barrier layer response, respectively [16]. The literature suggests that electrochemical results of AA2524 [17] or AA2024 clad [15] anodized, hydrothermally treated and sol-gel coated present only two peaks. However, the great amount of precipitates presented in the AA2024 T-3 can be responsible to the peak at medium frequencies, related to a sol-gel and defective porous hybrid layer. On the contrary of the results obtained for the anodized and unsealed samples - Fig. 3, the impedance values of anodized, hydrothermally treated and sol-gel coated samples increased after 336 h (2 weeks) of immersion, indicating that this phenomenon is related to the presence of Ce ions - Figs. 4 and 5. The increase of the impedance values could be explained by the presence of corrosion products or the self-healing of the protective layer. Fig. 8 shows that anodized and unsealed samples are corroded after 672 h of immersion in the test solution. However, the corrosion process could not be detected on the surface of the samples anodized, hydrothermally treated in Ce solution and sol-gel coated, even after 1008 h of electrochemical tests - Fig. 9. Thus, the variation of the impedance values was related to the self-healing of the protective layer, initiated by the corrosion process. Samples TSA anodized and hydrothermally treated using the same conditions described in this study were also evaluated (data not shown) to confirm that the improvement of the corrosion resistance was not related to the boehmite layer.

The EIS diagrams obtained for the anodized, hydrothermally treated and sol-gel coated samples were also fitted to electric equivalent circuits - Fig. 6c – presented one pair Rsg//CPEsg related to the sol-gel coating, other Rhl//CPEhl related to a hybrid layer formed by sol-gel and the defective porous hybrid layer and, at least, one Rb//CPEb related to the barrier layer. Representative plots are shown in Figs. 4 and 5, confirming the accuracy of the fittings.

The Rb and Rhl values are presented in Fig. 7. The hydrothermal treatment in a cerium solution and sol-gel coating increased the Rb values up to three orders of magnitude. Besides, not only the Rb values of the sol-gel coated samples increased after 336 h (2 weeks) of immersion in the test solution, but also the ones sealed for 10 min presented results in the same order of magnitude up to 1008 h (6 weeks).

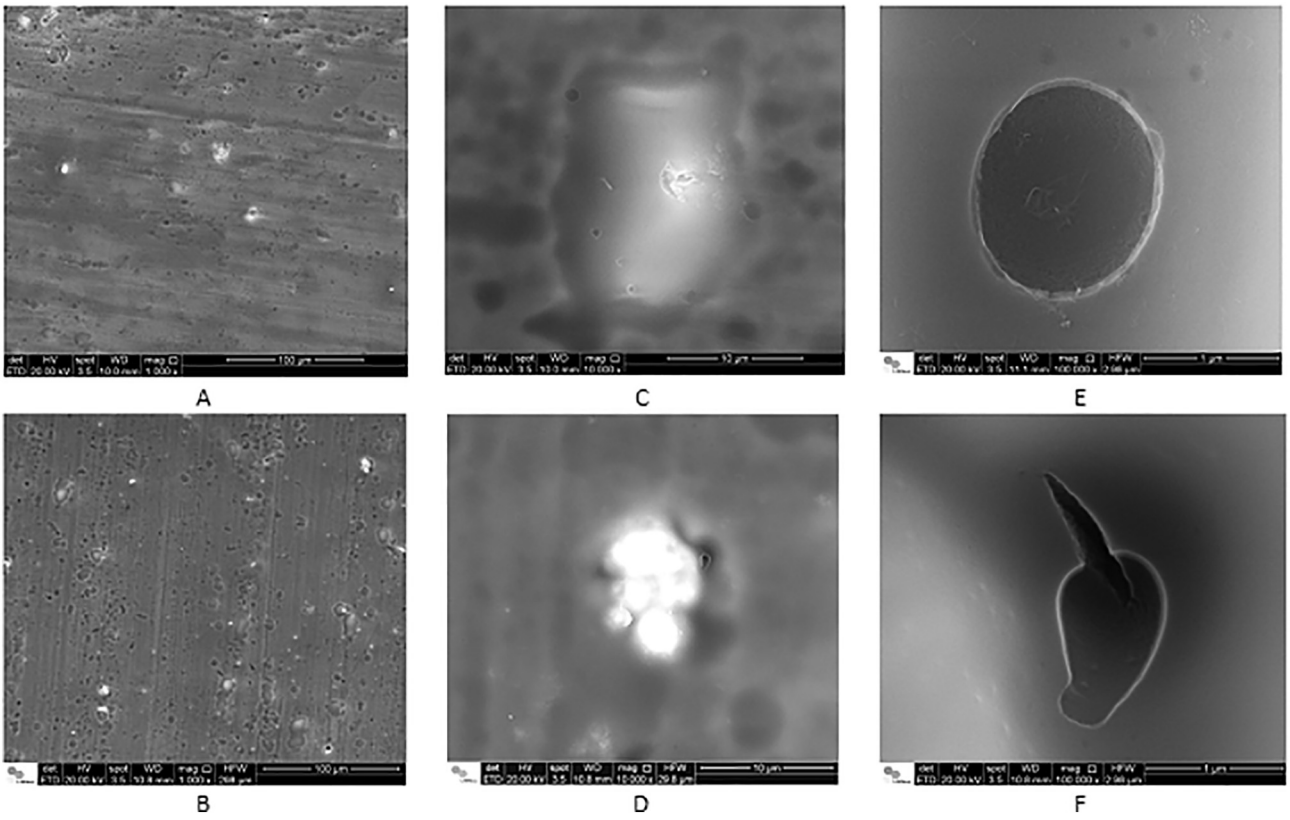

Fig. 9. FESEM images of AA2023-T3 TSA anodized, hydrothermally treated in Ce solution and sol-gel coated. (a), (c) and (e) wee hydrothermally treated for 5 min and (b), (d) and (f), for 10 min. After 1008 h of immersion in a naturally aerated 0.1 mol·L^{-1} NaCl solution.

The micrographs of the samples obtained after the EIS tests show that the hydrothermal treatment and the sol-gel coating improved the corrosion resistance of the anodized samples. Despite the roughness of the surface, even the defective areas were coated with sol-gel - Fig. 9. Corrosion products could not be noticed on the surface, nor around the intermetallics - Fig. 9e and f. These results suggest that the presence of the ions Ce in the hydrothermal treatment solution increased the corrosion resistance of the anodized samples of AA2024-T3.

5. Conclusions

The impedance values of both samples hydrothermally treated in Ce (III) solution increased after 336 h of immersion, suggesting that this ion was responsible by the self-healing process. Besides, the addition of Ce(III) ions to the hydrothermal treatment bath does not hinder the protective properties of the integrated sol-gel-boehmite protective layer. The sealing in the Ce(III) solution for 10 min presented better results than for 5 min.

The scanning electron microscopy results showed that the sol-gel layer increased the corrosion resistance of the TSA anodized AA2024-T3. However, presented pores and defects were detected around the intermetallics.

Acknowledgements

Authors acknowledge CAPES and CNPq (Proc. 4007810/2013-1) for the financial support to this work. Dr. Maysa Terada is grateful for the grant awarded (Proc. 1536157), Dr. Hellen Costenaro and Dr. Fernanda Martins Queiroz.

References

[1] J. Staley, D.L.-J.D.P. IV, undefined, Advances in Aluminum-Alloy Products for Structural Applications in Transportation, (1993) (… *ZI Court. AVE 7 AV* ….).
[2] S.J. Garcia-Vergara, K. El Khazmi, P. Skeldon, G.E. Thompson, Influence of copper on the morphology of porous anodic alumina, Corros. Sci. 48 (10) (2006) 2937–2946 Oct.
[3] F. Le Coz, L. Arurault, L. Datas, Chemical analysis of a single basic cell of porous anodic aluminium oxide templates, Mater. Charact. 61 (3) (2010) 283–288 Mar.
[4] J.W. Diggle, T.C. Downie, C.W. Goulding, Anodic oxide films on aluminum, Chem. Rev. 69 (3) (1969) 365–405.
[5] J. González, M. Morcillo, E. Escudero, V. López, E. Otero, Atmospheric corrosion of bare and anodized aluminium in a wide range of environmental conditions. Part I: visual observations and gravimetric results, Surf. Coat. Technol. 153 (2–3) (2002) 225–234. Apr.
[6] M.S. Donley, R.A. Mantz, A.N. Khramov, V.N. Balbyshev, L.S. Kasten, D.J. Gaspar, The self-assembled nanophase particle (SNAP) process: a nanoscience approach to coatings, Prog. Org. Coat. 47 (3–4) (2003) 401–415 Sep.
[7] S. Grieshop, Comparison of the Corrosion Behavior of High Strength Aluminum Alloys after Exposure to ASTM B117 Environment, (2014).
[8] H. Costenaro, et al., Corrosion resistance of 2524 Al alloy anodized in tartaric-sulphuric acid at different voltages and protected with a TEOS-GPTMS hybrid sol-gel coating, Surf. Coat. Technol. 324 (2017).
[9] M. García-Rubio, et al., Effect of postreatment on the corrosion behaviour of tartaric-sulphuric anodic films, Electrochim. Acta 54 (21) (2009) 4789–4800.
[10] H. Costenaro, F.M.F.M. Queiroz, M. Terada, M.-G.M.G. Olivier, I. Costa, H.G.H.G. De Melo, Corrosion protection of AA2524-T3 anodized in tartaric-sulfuric acid bath and protected with hybrid sol-gel coating, Key Eng. Mater. 710 (2016) 210–215.
[11] M. Terada, F.M. Queiroz, H. Costenaro, M. Olivier, I. Costa, H.G. De Melo, Effect of cerium (III) on the corrosion protection properties of the film formed on the AA2524-T3 alloy by hydrothermal treatments, Eurocorr 2016, 2016.
[12] M. Zemanová, P. Fellner, M. Chovancová, The preparation of combined aluminium oxide coatings on aluminium substrate, Chem. Pap. 50 (2) (1996) 55–59.
[13] F.M. Queiroz, Estudo do comportamento de corrosão dos intermetálicos presentes na liga aa2024-t3, por meio de técnicas de microscopia associadas a técnicas eletroquímicas, (2008).
[14] L. Fratila-Apachitei, J. Duszczyk, L. Katgerman, Voltage transients and morphology of AlSi(Cu) anodic oxide layers formed in H2SO4 at low temperature, Surf. Coat. Technol. 157 (1) (2002) 80–94. Aug.
[15] V.R. Capelossi, M. Poelman, I. Recloux, R.P.B. Hernandez, H.G. De Melo, M.G. Olivier, Corrosion protection of clad 2024 aluminum alloy anodized in tartaric-sulfuric acid bath and protected with hybrid sol-gel coating, Electrochim. Acta 124 (2014) 69–70.
[16] M.-E. Druart, et al., Influence of sol–gel application conditions on metallic substrate for optical applications, Corros. Eng. Sci. Technol. 46 (6) (2011) 677–684 Sep.
[17] H.C. Guadagnin, Corrosion Resistance Study of AA2524 Anodized in Sulphuric-Tartaric Acid and Sealed with Hybrid Coatings, (2017).